

# Indoor MIMO Channel Measurement and Modeling

Jesper Ødum Nielsen, Jørgen Bach Andersen

Department of Communication Technology  
Aalborg University  
Niels Jernes Vej 12, 9220 Aalborg, Denmark  
{jni,jba}@kom.aau.dk

**Abstract**—Forming accurate models of the multiple-input multiple-output (MIMO) channel is essential both for simulation as well as understanding of the basic properties of the channel. This paper investigates different known models using measurements obtained with a  $16 \times 32$  MIMO channel sounder for the 5.8 GHz band. The measurements were carried out in various indoor scenarios including both temporal and spatial aspects of channel changes. The models considered include the so-called Kronecker model, a model proposed by Weichselberger *et al.*, and a model involving the full covariance matrix, the most accurate model for Gaussian channels. For each of the environments different sizes of both the transmitter and receiver antenna arrays are investigated,  $2 \times 2$  up to  $16 \times 32$ . Generally it was found that in terms of capacity cumulative distribution functions (CDFs) all models fit well for small array sizes, but none of them are good for large arrays. Additionally, some results on stationarity of the channel are presented.

**Keywords**—MIMO channel measurements, indoor radio channel, MIMO modeling, stationarity, MIMO capacity

## I. INTRODUCTION

Future wireless communications devices are expected to offer bit rates of several hundred Mbit/s. This will require high spectral efficiencies of the transmission systems because the radio spectrum available for each pair of transceivers is limited. Systems using MIMO transmission techniques are promising in this aspect and has been studied intensely recently [1], [2]. However, the capacity of MIMO systems are highly dependent on the mobile channel properties [3], [4].

The focus of this work is MIMO transmission to and from mobile devices in an indoor environment where a large capacity is expected because of a generally high degree of signal scattering and lack of line of sight (LOS) in many cases. The mobile device may be a laptop or similar with sufficient space for many antennas and the device may be moving or remain stationary for periods of time. Hence, a variety of different channels may be experienced with varying degrees of stationarity, dispersion, *etc.* The current paper reports on results obtained from measurements with a 100 MHz wideband  $16 \times 32$  MIMO channel sounder for the 5.8 GHz band. The measurements are carried out in various indoor environments and includes both temporal and spatial aspects of channel changes.

Forming accurate models of the MIMO channel is essential both for system simulation as well as understanding of the basic properties of the channel. It is well known that the simple so-called Kronecker model is inaccurate in some situations [5], and other potentially more accurate models have been suggested, such as the Weichselberger model [6] and a model recently proposed by Andersen [7]. In the current work different models are compared for widely varying indoor environments and

using different size and geometries of both the transmitter and receiver antenna arrays. The comparison includes a model using the full covariance matrix of all the transmitter/receiver channel combinations, which is an accurate model assuming Gaussian statistics of the channel coefficients. However, in general the channel cannot be assumed Gaussian. The models are compared in terms of channel capacity.

## II. MEASUREMENTS

The measured data used in the current work is obtained using a MIMO channel sounder operating at a carrier frequency of 5.8 GHz. The sounder uses the correlation principle, where the correlation is carried out in a post processing procedure after the received signals have been sampled. By transmitting independent streams of pseudo noise (PN) sequences, the sounder measures 16 transmit channels simultaneously. Each transmit branch use a 1 W power amplifier. On the receive side four channels were measured in parallel, and using switching each branch is extended so that in total 32 receive channels are measured. Additional information about the sounder is available in [8].

The full  $16 \times 32$  MIMO channel is measured in a time-triggered way at a rate of 60 Hz, corresponding to a theoretical maximum relative mobile speed of about 1.5 m/s, assuming a maximum Doppler shift given by  $f_{\max} = v/\lambda$  where  $v$  is the mobile speed and  $\lambda$  is the wavelength. Each measurement of the complex MIMO channel takes about 1.3 ms with the current setup.

As part of the post-processing procedure the measurements are compensated for the sounder system response, obtained from back-to-back measurements of all combinations of transmit and receive channels. In this process the sounding bandwidth is limited to about 100 MHz.

All measurements were made using planar arrays of monopole antenna elements arranged in a rectangular grids with a spacing of 2.5 cm, or  $0.48\lambda$ . The arrays have two rows of dummy elements on all array edges, which are not used but terminated as the active elements. For the transmitter array the active elements are arranged in a  $4 \times 4$  grid while the receiver array is  $4 \times 8$ .

During measurements the transmitter array is moved along a horizontal half-circular path with a radius of about 0.5 m. The speed along the arc is about 52 mm/s or about one  $\lambda/s$ . The transmitter array and the device for movement is depicted in Fig. 1. The distance from the array ground plane to the floor is about 90 cm.

Simultaneously with the transmitter array movements, the receiver array is moved linearly while the measurements take

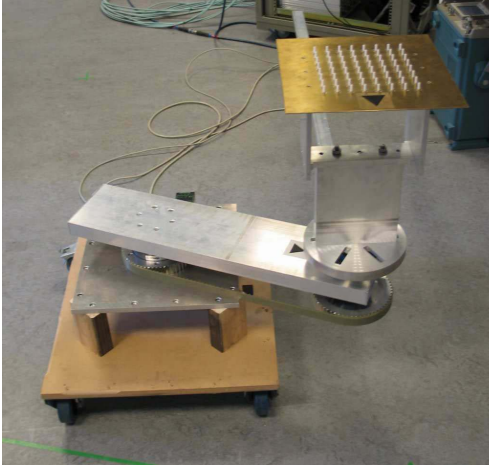


Fig. 1. The pedestal for circular movement of the transmitter array including the  $4 \times 4$  planar array of monopole elements with dummy elements. The element spacing is 2.5 cm.

place, at a speed of about 30 mm/s corresponding to about  $0.6\lambda/s$ . The distance from the array ground plane to the floor is 94 cm.

It is important to notice that due to the dummy elements of both the transmitter and the receiver array, the main beams of the radiation patterns for the individual elements are elevated about  $45^\circ$  from the ground plane. At elevation angles close to  $0^\circ$  the attenuation is about 20 dB compared to the main direction.

All the measurements were made within the same modern four story (including basement) office building. The building is primarily made of reinforced concrete with an outer brick wall and with most inner partitions made in light plaster board construction. The floors/ceilings of each level are also made of concrete.

The measurement campaign was divided into a number of different scenarios, described in the following subsections.

#### A. Open Lab

In this scenario both transceivers are located inside or nearby a large room, containing much furniture and equipment, including bookshelves and room partitioning that may block the LOS between the transmitter (Tx) and receiver (Rx). In addition people activity can be expected in this room. For all of these measurements the Tx array was located in the corridor next to the open lab environment, but LOS was blocked in all cases. The main part of the lab has dimensions of about  $13 \text{ m} \times 7 \text{ m}$ .

The Rx antenna array was located in different places around the Tx. For the current work two of measurements from this scenario are included, labeled ‘L2’ and ‘L5’;

**L2:** The array is located in the south end of the main lab room.

**L5:** The array is located inside a room next to the main lab, with the door between open.

#### B. Office to Office

In this scenario both the Tx and Rx arrays are located inside small offices next to the 2nd floor corridor.

**O1:** The offices are on opposite sides of the corridor with about 10 m between the offices, but with non-line of sight (NLOS), due to a bend of the corridor.

**O3:** The offices are next to each other on the same side of the corridor.

#### C. Building Level Crossing

For these measurements the Tx array is on the 1st floor and the Rx is on the 2nd floor. In this situation most of the energy can be expected to propagate via corridors and staircases. The two floors are connected to a main entrance hall which covers the full height of the building. The Tx array is in the same location for the following two Rx scenarios,

**V1:** The Rx is inside an office next to the 2nd floor corridor.

**V3:** The Rx is in the 2nd floor corridor.

#### D. Basement

In this case both the Tx and the Rx are located inside the same large room on the basement floor. This is a storage room which has concrete floor, ceiling and walls where the ceiling is cluttered with various pipes, lamps, *etc.* The room joins a corridor in one side. For the measurements selected for the current work the Tx is located in a the south-east corner of the room and the Rx is at two different positions in the corridor:

**B1:** Rx at south-west, near NLOS condition.

**B5:** Rx in corridor north of room, NLOS condition.

In addition to the channel changes introduced by the movements of the transceivers, other changes in the channel can also be expected since the measurements were carried out while normal work activity in the building took place.

### III. MIMO CHANNEL MODELS

In the following a narrowband channel is assumed so that the received signal can be described as  $\mathbf{y} = \mathbf{H}\mathbf{s} + \mathbf{n}$ , where  $\mathbf{s}$  is the vector of transmitted symbols with length  $M$ ,  $\mathbf{n}$  is a same size noise vector, and  $\mathbf{H}$  is the  $N \times M$  random channel matrix.

It is convenient to assume that the elements of  $\mathbf{H}$  are zero-mean complex Gaussian distributed, leading to following model of the MIMO channel,

$$\text{vec}(\mathbf{H}_{\text{Full}}) = \mathbf{R}_H^{1/2} \text{vec}(\mathbf{G}) \quad (1)$$

where the  $\text{vec}(\cdot)$  operation stacks the columns of the matrix argument into one column vector,  $\mathbf{G}$  is a  $N \times M$  matrix of zero mean, independent random Gaussian values, and  $\mathbf{R}_H = \mathcal{E}[\text{vec}(\mathbf{H})\text{vec}(\mathbf{H})^H]$  is the full covariance matrix of the channel. The ‘ $\mathcal{E}\{\cdot\}$ ’ operator denotes statistical expectation. Under the Gaussian assumption, the model in (1) is the most comprehensive but also has the drawback of requiring knowledge of the full correlation matrix.

In the so-called Kronecker model [9] it is assumed that the correlations between receiver antenna elements are independent of the transmit antenna, and vice versa the correlations between transmitter antenna elements are independent of the receiver antenna. This simplifies the complete correlation matrix which in this case may be written as  $\mathbf{R}_H = \mathbf{R}_{\text{Tx}} \otimes \mathbf{R}_{\text{Rx}}$  where ‘ $\otimes$ ’ denotes the matrix Kronecker product, and where  $\mathbf{R}_{\text{Tx}} = \mathcal{E}\{\mathbf{H}^T \mathbf{H}^*\}$  and  $\mathbf{R}_{\text{Rx}} = \mathcal{E}\{\mathbf{H}\mathbf{H}^H\}$  are the transmitter and receiver correlation matrices, respectively. The Kronecker MIMO channel may be simulated as

$$\mathbf{H}_{\text{Kron}} = P^{-1/2} \mathbf{R}_{\text{Rx}}^{1/2} \mathbf{G} \left( \mathbf{R}_{\text{Tx}}^{1/2} \right)^T \quad (2)$$

in which  $\mathbf{G}$  contains random Gaussian values as above and  $P$  is a normalization term.

The assumptions behind the Kronecker model may be too restrictive and therefore another model has been proposed in which the correlation matrices for the receiver antennas are not assumed independent of the transmitter antenna, and the correlation matrices for the transmitter antennas are not independent of the receiver antennas. In the model proposed by Weichselberger *et al* [6] these matrices share the same eigenbasis but may vary in eigenvalues and hence some variation is allowed. In this model the channel is simulated as follows

$$\mathbf{H}_{\text{Weich}} = \mathbf{U}_{\text{Rx}} (\tilde{\mathbf{\Omega}} \odot \mathbf{G}) \mathbf{U}_{\text{Tx}}^T \quad (3)$$

with ' $\odot$ ' denoting element-wise multiplication. The elements of the  $\tilde{\mathbf{\Omega}}$  matrix are given by

$$\tilde{\Omega}_{m,n} = \left[ (\mathbf{u}_{\text{Tx},m} \otimes \mathbf{u}_{\text{Rx},n})^H \mathbf{R}_H (\mathbf{u}_{\text{Tx},m} \otimes \mathbf{u}_{\text{Rx},n}) \right]^{1/2} \quad (4)$$

where  $\mathbf{u}_{\text{Tx},m}$  is the  $m$ 'th eigenvector of  $\mathbf{R}_{\text{Tx}}$  and  $\mathbf{U}_{\text{Tx}}$  is the matrix containing the complete eigenbasis. Similarly,  $\mathbf{u}_{\text{Rx},n}$  is the  $n$ 'th eigenvector of  $\mathbf{R}_{\text{Rx}}$  and  $\mathbf{U}_{\text{Rx}}$  is the complete eigenbasis of  $\mathbf{R}_{\text{Rx}}$ .

All of the models presented above results in Gaussian statistics of  $\mathbf{H}$ . The model in [7] is a double bounce model allowing non-Gaussian statistics. However, this model is not discussed further here.

#### IV. RESULTS

Assuming that the transmitter has no knowledge of the channel, the capacity of the channel is given by [2]

$$C = \sum_{i=1}^R \log_2 \left( 1 + \frac{\rho}{M} \lambda_i \right) \quad (5)$$

where  $\rho$  is the signal to noise ratio (SNR),  $R = \min\{M, N\}$  and  $\lambda_i$  is the  $i$ 'th eigenvalue of the matrix

$$\mathbf{W} = \begin{cases} \mathbf{H}\mathbf{H}^H, & N \leq M \\ \mathbf{H}^H\mathbf{H}, & M < N \end{cases} \quad (6)$$

Since it is dependent on the random channel matrix  $\mathbf{H}$ , the capacity it is a random variable and must be characterized in statistical terms. In the following the capacity is computed for each instantaneous measured or simulated channel, and CDFs are computed.

Although the measurements are wideband all results in the current paper are computed from narrowband data, which is obtained by using a single frequency bin after transforming to the frequency domain. Before computing capacity and estimating covariance matrices, the power of the measured  $\mathbf{H}$  matrices have been normalized for each measured position, where the power is estimated using the average over all  $16 \times 32$  Tx and Rx antenna combinations, corresponding to averaging in space.

In the following the first 600 MIMO channel measurements of each measurement series are used for analysis, corresponding to 10 s or about 10 wavelengths of movement in space for the Tx array. Initially this distance was assumed to be sufficiently short to justify an assumption of a stationary channel and, on the other hand, the distance covered should be large enough to allow for a proper averaging. This issue is discussed further below.

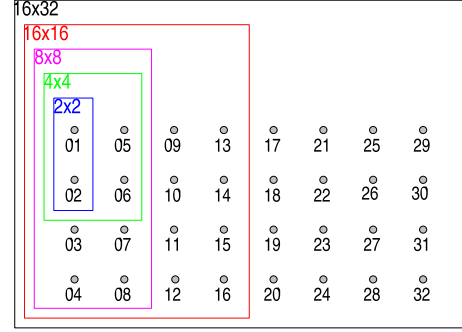


Fig. 2. The different sub-array selections, shown for the Rx array. The selection was similar for the Tx array, except for it being half the size.

Fig. 3 shows CDF curves for the capacities computed from the channel measurements made in four different environments, in each case with five different array geometries and sizes, as illustrated in Fig. 2. The capacity is in all cases computed for an SNR of 10 dB where the signal power is computed as an average over all Tx/Rx antenna combinations and measured positions.

Also shown in Fig. 3 are the CDF curves for each of the models described in Sec. III. For each measurement the covariance matrix is estimated based on the 600 measurements and the channel is simulated according to (1), (2), and (3). In all cases 600 MIMO channels are simulated.

In general the match between the CDFs for the simulated and the measured channels gets better for smaller array constellations, with a nearly perfect match in some cases for a  $2 \times 2$  constellation. However, for large arrays the match between the curves for measured data and the models is rather poor, although in some cases not shown here a better match exists. Furthermore, it is interesting to note that the slope of the curve for the full covariance matrix model is different from those for the remaining models and perhaps closer to the CDF for the measured data.

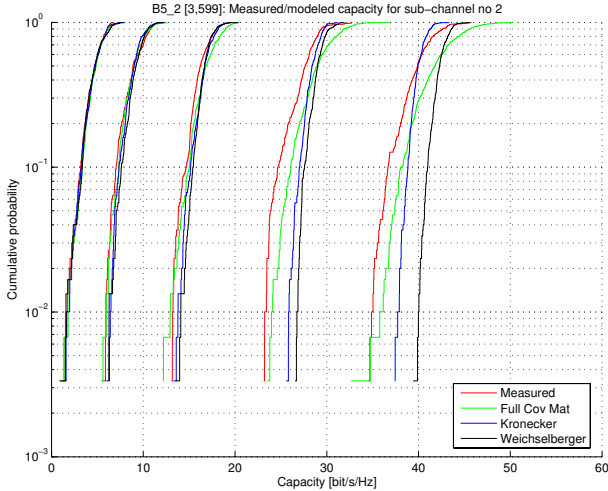
Fig. 3 only shows results for some of the measured environments. The mean capacities for all the measured environments are shown in Fig. 4 for different array constellations, and Fig. 5 shows the mean capacities of both the measured and modeled channels for the  $16 \times 32$  array constellation.

The curves in Fig. 3 for, *e.g.*, the measured O3 environment are somewhat different from most of the environments. Fig. 6 shows the capacity for this environment versus measurement position, where the capacity evolves from a rather stable capacity in the first 300 position to a somewhat higher level in the last positions. This suggests a non-stationary channel, which is supported by the curve for the average received power. Note, however, that the capacity was computed using normalized channels.

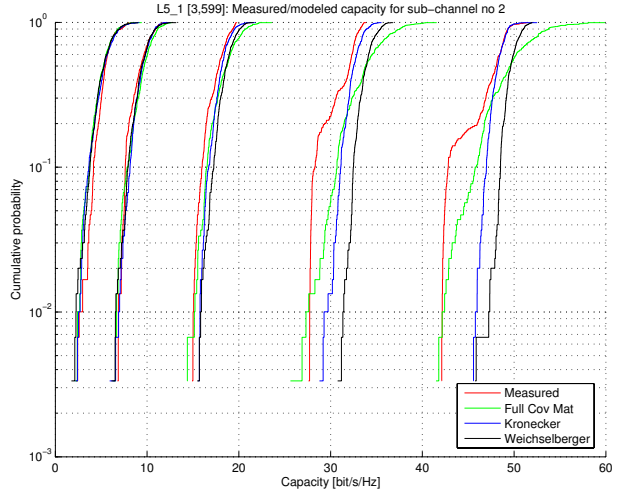
If the SNR is sufficiently high the capacity in (5) may be approximated as [7]

$$C \simeq 0.33 R \cdot \left( \frac{\rho}{M} \right)_{\text{dB}} + \sum_{i=1}^R \log_2(\lambda_i) \quad (7)$$

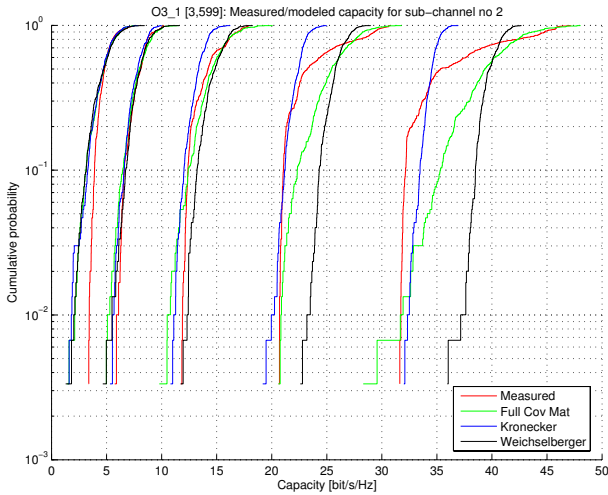
where it is noticed that the first term depends only on the SNR and the number of antennas, while the second term is channel



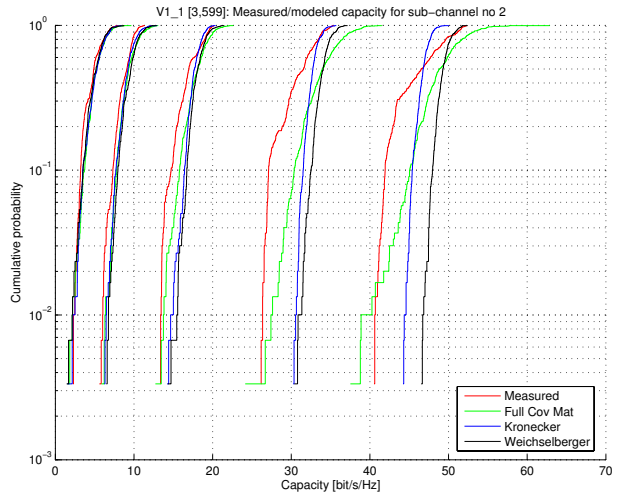
(a) Basement environment (B5)



(b) Lab environment (L5)



(c) Office-to-office environment (O3)



(d) Level-to-level environment (V1)

Fig. 3. CDF curves for capacity in different measured environments and associated models. From left to right, the groups of curves are for array constellations ( $T_x \times R_x$ )  $2 \times 2$ ,  $4 \times 4$ ,  $8 \times 8$ ,  $16 \times 16$ ,  $16 \times 32$ .

related. The *richness* was defined in [7] as

$$R(k) = \sum_{i=1}^k \log_2(\lambda_i) \quad (8)$$

where it is assumed that the eigenvalues are sorted in descending order. The richness is a convenient way of showing some of the essential channel properties. In Fig. 7 the mean richness curves for measurement position 1–250 and 351–600 are shown, supporting the notion that essential properties of the channel changes and hence is non-stationary.

## V. CONCLUSION

The current work is based on MIMO channel measurements in widely different indoor scenarios. Depending on the environment, mean capacities of 35–50 bit/s/Hz were observed,

assuming an SNR of 10 dB and a  $16 \times 32$  array constellation. The measured channels were simulated using the Kronecker, full covariance matrix, and Weichselberger models and compared in terms of cumulative distribution functions (CDFs) of the capacities. For small array constellations the fit is excellent, but for large arrays the discrepancies may be large. The measurements were conducted with moving transceiver arrays to allow for averaging. In some cases it appears that the channel may be non-stationary even within surprisingly small areas of movements. However, this is observable only for large arrays, since the differences are mainly observed when many eigenvalues are involved.

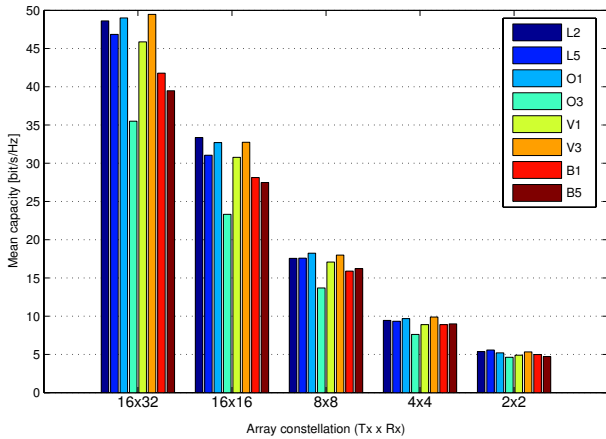


Fig. 4. Mean capacity for measured data from different environments and for different array constellations. The SNR is 10 dB.

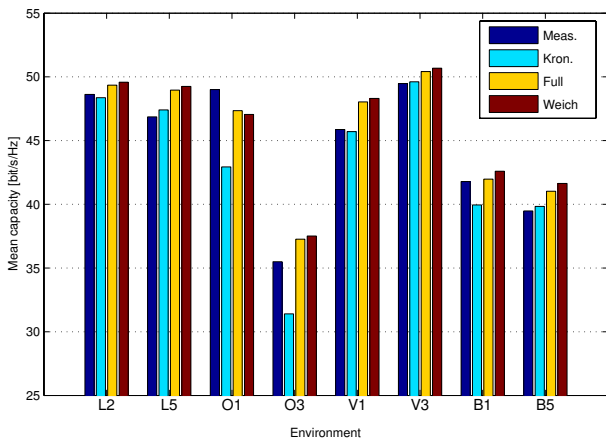


Fig. 5. Mean capacity for measured and simulated channel data from different environments, assuming a  $16 \times 32$  array constellation and an SNR of 10 dB.

#### ACKNOWLEDGMENT

Financial and technical support received from DoCoMo Euro-Labs is gratefully acknowledged.

#### REFERENCES

- [1] G.J. Foschini and M. J. Gans, "On limits of wireless communications in a fading environment when using multiple antennas," *Wireless Personal Communications*, vol. 6, no. 3, pp. 311–335, Mar. 1998.
- [2] David Gesbert, Mansoor Shafi, Da shan Shiu, Peter J. Smith, and Ayman Naguib, "From theory to practice: An overview of MIMO space-time coded wireless systems," *IEEE Journal on Selected Areas in Communications*, vol. 21, no. 3, pp. 281–302, Apr. 2003.
- [3] M. Herdin, H. Özcelik, H. Hofstetter, and E. Bonek, "Variation of measured indoor MIMO capacity with receive direction and position at 5.2 GHz," *Electronics Letters*, vol. 38, no. 21, pp. 1283–1285, Oct. 2002.
- [4] J.W. Wallace, M.A. Jensen, A.L. Swindlehurst, and B.D. Jeffs, "Experimental characterization of the MIMO wireless channel: data acquisition and analysis," *IEEE Transactions on Wireless Communications*, vol. 2, no. 2, pp. 335–375, Mar. 2003.
- [5] H. Özcelik, M. Herdin, W. Weichselberger, J. Wallace, and Ernst Bonek, "Deficiencies of 'Kronecker' MIMO radio channel model," *Electronics Letters*, vol. 39, no. 16, pp. 1209, 2003.

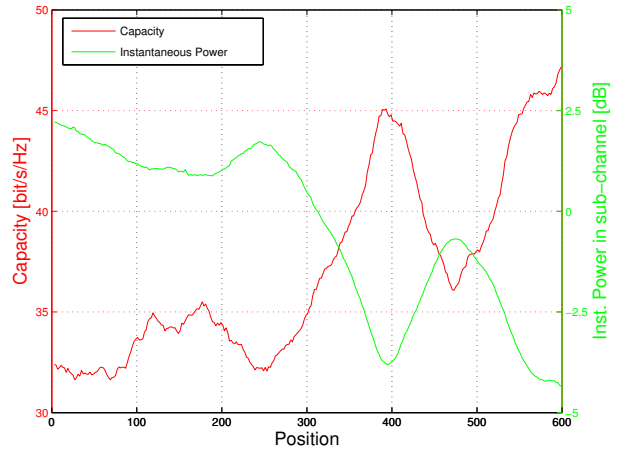


Fig. 6. Capacity versus position (left axis), and instantaneous power (right axis). Results for the O3 environment, assuming a  $16 \times 32$  array constellation and an SNR of 10 dB.

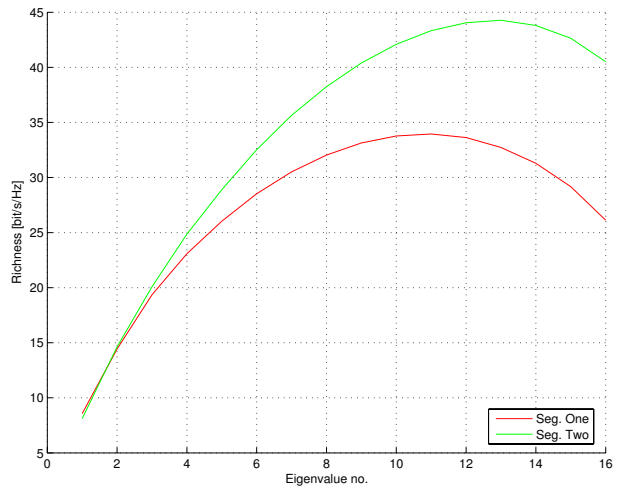


Fig. 7. Richness for the O3 measurement environment. The two curves show the mean richness curve for measurement position 1–250 and 351–600, respectively.

- [6] Werner Weichselberger, Hüseyin Özcelik, Markus Herdin, and Ernst Bonek, "A novel stochastic MIMO channel model and its physical interpretation," in *The Proceedings of the 6th International Symposium on Wireless Personal Multimedia Communications (WPMC'03)*, 2003.
- [7] J. Bach Andersen and J. Ødum Nielsen, "Modelling the full MIMO matrix using the richness function," in *Proceedings of the ITG/IEEE Workshop on Smart Antennas (WSA) 2005*, Apr. 2005.
- [8] J. Ø. Nielsen, J. B. Andersen, P. C. F. Eggers, G. F. Pedersen, K. Olesen, E. H. Sørensen, and H. Suda, "Measurements of indoor  $16 \times 32$  wideband MIMO channels at 5.8 GHz," in *Proceedings of the 2004 International Symposium on Spread Spectrum Techniques and Applications (ISSSTA 2004)*, 2004, pp. 864–868.
- [9] Jean Philippe Kermoal, Laurent Schumacher, Klaus Ingemann Pedersen, Preben Elgaard Mogensen, and Frank Frederiksen, "A stochastic MIMO radio channel model with experimental validation," *IEEE Journal on Selected Areas in Communications*, vol. 20, no. 6, pp. 1211–1226, 2002.